Available online at www.sciencedirect.com
ScienceDirect
Catalysis Today 118 (2006) 113–120
CATALYSIS TODAY
www.elsevier.com/locate/cattod

Competitive diffusion and adsorption in Vycor glass membranes—A lumped parameter approach

E.-U. Schlünder [a], J. Yang [a,b], A. Seidel-Morgenstern [a,c,*]

[a] Max-Planck-Institute Dynamics of Complex Technical Systems, D-39106 Magdeburg, Germany
[b] Dalian Institute of Chemical Physics, Chinese Academy of Sciences, 116023 Dalian, PR China
[c] Otto-von-Guericke-Universität, D-39106 Magdeburg, Germany

Available online 7 July 2006

Abstract

The interaction of simultaneous diffusion and adsorption of pure gases and gas mixtures in a Vycor glass membrane has been studied under transient conditions in a modified Wicke–Kallenbach cell. A lumped two parameter approach was developed in order to analyse all the observed pressure responses in a unified manner. This approach was found to be capable to fit well almost all the observations made for different types of gases and at different temperatures with sufficient or excellent accuracy.

Keywords: Vycor glass membrane; Langmuir adsorption isotherm; Knudsen diffusion

1. Introduction

In order to use membranes successfully in separation processes and in membrane reactors, the rate of transport should be known [1,2]. This study is devoted to quantify the transport rate in a porous glass possessing interesting properties. Vycor glass applied for measurements was already used in the previous studies [3–6]. It consists of 96% silica with the remainder to be mainly B_2O_3.

The average pore diameter of Vycor glass is approximately 4 nm. The pore size distribution is relatively narrow. The glass strongly adsorbs many organic and inorganic gases. Vycor glass membranes can be used for gas separation and dosing processes with and without simultaneous reactions. The understanding of mass transfer through the membranes is essential for successful applications.

The modified dynamical Wicke–Kallenbach diffusion cell [7] is an effective approach to investigate the mass transfer in a porous medium such as in solid adsorbents and catalysts and membranes. Do et al. [8] simulated the transient pressure response at the downside reservoir to quantify mass transfer of hydrocarbons as single component system in activated carbons by taking into account gas phase diffusion and adsorption. Dogan and Dogu [9] analysed the dynamics of flow and diffusion of adsorbing tracers in Al_2O_3 and Pd–Al_2O_3 pellets using a pulse-response technique. In previous works, the generalized Maxwell–Stefan theory [10] was applied to study gas phase diffusion and surface diffusion in Vycor glass [4,5]. A relatively good description of coupled gas phase and surface diffusion was achieved for experiments with single components or with binary mixtures of inert gases. Less effort was devoted to study the behaviour of mixtures of adsorbable gases.

In this work the interplay between simultaneous diffusion and adsorption of pure gases and gas mixtures has been studied using a modified Wicke–Kallenbach cell, which consists out of two chambers and which was operated under transient conditions. In the pore size range of Vycor glass for light gases, such as He, N_2, CO_2, and small hydrocarbons, like C_3H_8 and C_4H_{10}, the mean free path length at atmospheric pressure and temperature is much larger than the pore width ($\lambda/d_{pore} > 10$) [11]. Thus, contributions of bulk molecular diffusion and viscous flow to overall mass transfer are small and can be ignored. If two gases cross the membrane counter-currently with different velocities the pressure within one chamber changes as a function of time. Several pressure responses were measured with different gases and at various temperatures.

In contrast to the relatively complicated Stefan–Maxwell equations mentioned above, a simple two parameter equation –

* Corresponding author. Tel.: +49 391 6110 401; fax: +49 391 6110 403.
E-mail address: seidel-morgenstern@mpi-magdeburg.mpg.de
(A. Seidel-Morgenstern).

0920-5861/$ – see front matter © 2006 Elsevier B.V. All rights reserved.
doi:10.1016/j.cattod.2005.11.094

Nomenclature

A	surface area of the membrane (m^2)
b_i	parameter in the Langmuir adsorption isotherm (bar^{-1})
c	total concentration in the open volume (mol m^{-3})
c_1	concentration of component 1 in the closed volume (mol m^{-3})
c_2	concentration of component 2 in the closed volume (mol m^{-3})
$D_{K,i}$	Knudsen diffusivity of component i (m^2 s^{-1})
$D_{s,i}$	surface diffusivity of component i (m^2 s^{-1})
$F_{cap,i}$	storage capacity enlargement factor
$F_{Diff,i}$	permeability enchancement factor
G	volumetric flow rate (m^3 s^{-1})
i	component i, $i = 1, 2$
K_0	Knudsen coefficient (m)
M_i	molecular weight (g mol^{-1})
N_1	diffusive molar flow rate of component 1 (mol s^{-1})
N_2	diffusive molar flow rate of component 2 (mol s^{-1})
p_i	partial pressure of component i (Pa)
ΔP	pressure difference between outer and inner volume (Pa)
P_{ex}	total pressure in the open side of the membrane (Pa)
q_i	adsorbed phase concentration of component i (mmol m^{-3})
q_{sat}	total saturation capacity of adsorbed species (mmol m^{-3})
Q	amount adsorbed in the membrane (mol)
R	universal gas constant (J mol^{-1} K^{-1})
S_m	length of the Vycor membrane (m)
t	time (s)
$t.1$	fitted relaxation time of component 1 (s)
$t.2$	fitted relaxation time of component 2 (s)
$t_{1,k}$	calculated relaxation time of component 1 by Knudsen diffusion (s)
$t_{2,k}$	calculated relaxation time of component 2 by Knudsen diffusion (s)
V	volume of the closed chamber (m^3)
V_m	specific pore volume of the membrane (m^3)
$V_{m,s}$	average saturated pore volume of the membrane (m^3)
$y_{1,ex}$	molar fraction of component 1 in the open volume
$y_{2,ex}$	molar fraction of component 2 in the open volume
$y_{1,0}$	initial molar fraction of component 1 in the diffusion cell

Greek letters

β_1	permeability of component 1 (m s^{-1})
β_2	permeability of component 2 (m s^{-1})
ε	porosity
γ_i	saturation factor of pore volume of the membrane
τ	tortuosity

which applies rigorously in case of pure Knudsen type diffusion – is suggested to describe the observations made using binary mixtures of non-adsorbable and adsorbable gases. The relation between the parameters determined and conventional transport coefficients is elucidated.

2. Experimental

The glass membrane provided by CORNING Inc. (USA) is originally opalescent and gradually turns brown during its exposition to the atmosphere. It was cleaned by heating in a solution of 30% hydrogen peroxide at 60 °C over night until the contaminating color disappears. Before measurements, the glass membrane was activated firstly by drying in nitrogen flowing over night at room temperature and then by heating at 180 °C for 2 h. The activation treatment removes absorbed water from the pore surface, therefore, disturbances due to moisture can be excluded.

A schematic illustration of the set-up is shown in Fig. 1. The temperature of the cell is kept constant. A large amount of sweep gas kept at constant ambient pressure and constant concentration flows past one side of the membrane (Fig. 1b) which is open to the atmosphere, while the other side of the membrane (Fig. 1c) is capsulated by a closed chamber with volume V. Before starting the measurement, the cell volume (Fig. 1a–c) is completely equilibrated with gas 1. At the beginning of the measurement, gas 1 is replaced by gas 2 by switching the four-way valve. The total pressure difference between the closed outer volume (Fig. 1c) and the open inner volume (Fig. 1b), $\Delta P(t)$, is recorded as a function of time. The exchange experiments were performed for the gases He/N_2; He/C_3H_8; He/C_4H_{10} at 20 °C, and for C_3H_8/CO_2 at various temperatures (20, 70, 120, 160 °C). The measurements were also conducted for C_3H_8/CO_2 mixtures with varying compositions. The accuracy of the pressure was about ±3% based on the pressure detector and temperature controller performance.

3. Simplified model: a lumped parameter approach

3.1. Prediction of transients

A lumped parameter approach is suggested for the prediction of the pressure difference between both chambers

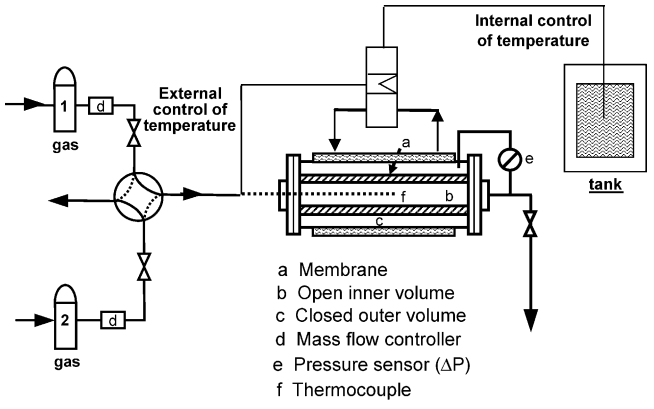

Fig. 1. Schematic illustration of set-up.

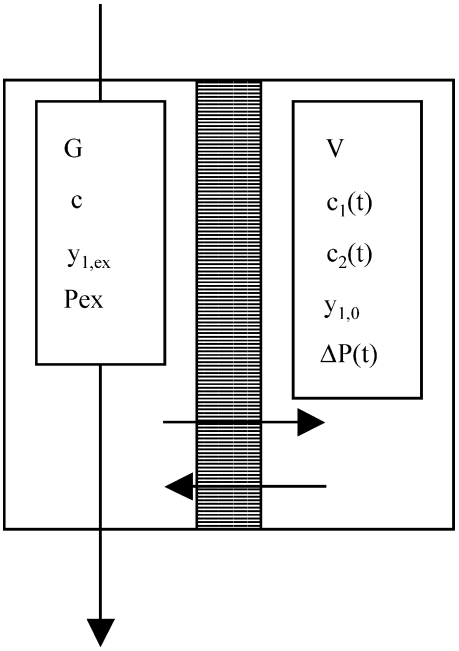

Fig. 2. Simplified scheme of diffusion cell and notation.

of the diffusion cell $\Delta P(t)$. The notation is introduced in Fig. 2. The following assumptions are made:

1. $c = P_{ex}/RT$ = constant.
2. Large sweep gas flow G, i.e. $y_{1,ex}$ = constant.
3. Permeabilities β_1 and β_2 are constant.
4. The fluxes N_1 and N_2 are independent of each other and are driven by linear concentration differences.
5. At $t = 0$: $P(t) = P_{ex}$.
6. Initial mol-fraction in the closed chamber: $y_{i,0}$.
7. Binary mixtures are used, $i = 1, 2$.

The model is based on the following equations:

$$N_1 = A\beta_1(cy_{1,ex} - c_1) \quad \text{(Flux 1)} \tag{1}$$

$$N_2 = A\beta_2(cy_{2,ex} - c_2) \quad \text{(Flux 2)} \tag{2}$$

$$N_1 = V\frac{dc_1}{dt} \quad \text{(Accumulation 1)} \tag{3}$$

$$N_2 = V\frac{dc_2}{dt} \quad \text{(Accumulation 2)} \tag{4}$$

This gives two independent linear differential equations:

$$\frac{dc_1}{dt} = \frac{cy_{1,ex} - c_1}{t.1} \tag{5}$$

$$\frac{dc_2}{dt} = \frac{cy_{2,ex} - c_2}{t.2} \tag{6}$$

$$t.1 = \frac{V}{A\beta_1} \quad \text{(relaxation time 1)} \tag{7}$$

$$t.2 = \frac{V}{A\beta_2} \quad \text{(relaxation time 2)} \tag{8}$$

Integration of Eqs. (5) and (6) gives

$$\frac{c_1}{c} = y_{1,ex} - (y_{1,ex} - y_{1,0})\exp\left(\frac{-t}{t.1}\right) \tag{9}$$

$$\frac{c_2}{c} = y_{2,ex} - (y_{2,ex} - y_{2,0})\exp\left(\frac{-t}{t.2}\right) \tag{10}$$

This leads to the following equation to describe the transient of the pressure difference between the two chambers:

$$\Delta P(t) = P_{ex}\left(\frac{c_1 + c2}{c - 1}\right) \tag{11}$$

or

$$\frac{\Delta P(t)}{P_{ex}} = (y_{1,ex} - y_{1,0})\left[\exp\left(-\frac{t}{t.2}\right) - \exp\left(-\frac{t}{t.1}\right)\right] \tag{12}$$

The maximum pressure difference occurs at t_{max} with

$$t.1\exp\left(\frac{-t_{max}}{t.2}\right) = t.2\exp\left(\frac{-t_{max}}{t.1}\right) \tag{13}$$

3.2. Interpretation of the relaxation time

3.2.1. Case 1: non-adsorbable gases

The assumptions 3 and 4 hold if the diffusion mechanism is of pure Knudsen type and no gas adsorption does occur. Then the permeabilities β_i follow from

$$\beta_i = \frac{4}{3}K_0\frac{v_i}{s_m}$$

$v_i = \sqrt{8RT/\pi M_i}$, Maxwell velocity with M_i being the molar weight while s_m is membrane thickness.

In the later section the relaxation time, where the gas transfer is governed by pure Knudsen diffusion is designated as Knudsen relaxation time, $t_{i,K}$, which can be written as

$$t_{i,K} = \frac{V}{A\beta_i} = \frac{VS_m}{A\frac{4}{3}K_0\sqrt{\frac{8RT}{\pi M_i}}} \tag{14a}$$

where $K_0 = d_P\varepsilon/(\tau/4)$ with d_P being the pore diameter, ε the membrane porosity and τ the tortousity factor. K_0 has to be calibrated by noble gas experiments.

3.2.2. Case 2: adsorbable gases

If gas adsorption does occur, two effects come into play. First, the storage capacity of the gas volume V is enlarged by the additional storage capacity of the membrane hold up. Second, the adsorbed gas enhances the mobility of the permeating species due to the fact that gas diffusion is accompanied by surface diffusion.

In a first order lumped parameter approximation the gas volume capacity can be modified by introducing an enlargement factor $F_{cap,i}$ and the permeability can be modified by introducing an enhancement factor $F_{diff,i}$.

Thus the modified relaxation times take the form

$$t.i = \frac{V}{A\beta_i}\frac{1+F_{\mathrm{cap},i}}{1+F_{\mathrm{Diff},i}}, \quad i=1,2 \tag{14b}$$

3.2.2.1. Case 2.1: inert gas (1)–adsorbable gas (2). The case is considered that component 1 will not be adsorbed (like He, Ar, N_2), while the adsorption of component 2 (CO_2, C_3H_8, C_4H_{10}) is assumed to be of Langmuir type:

$$Q = \frac{V_{\mathrm{m}} q_{\mathrm{sat}} bRTc_2}{1+bRTc_2} \tag{15}$$

The derivative writes

$$\mathrm{d}Q = \frac{V_{\mathrm{m}} q_{\mathrm{sat}} bRT}{(1+bRTc_2)^2}\mathrm{d}c \tag{16}$$

with c_2 being the local and time dependent concentration within the membrane.

An approximate solution for the lumped parameter approach can be obtained if a linear c_2 profile is assumed in the membrane. Considering the fact that at $t=0$, $c_2=c$ and at $t=\infty$, $c_2=0$, c_2 in Eq. (15) is set equal to $0.5c$. Due to this assumed average pressure in the membrane, the average saturated membrane volume $V_{\mathrm{m,s}}$ is corrected by factor γ_i, and can be expressed by $V_{\mathrm{m,s}} = \gamma_i V_{\mathrm{m}}$. ($V_{\mathrm{m}}$ is the membrane volume.) Thus Eq. (16) can be arranged as

$$\mathrm{d}Q = \frac{\gamma_2 V_{\mathrm{m}} q_{\mathrm{sat}} bRT}{(1+0.5bP_{\mathrm{ex}})^2}\mathrm{d}c_2 \tag{17}$$

This leads to the capacity enlargement factor for the adsorbable component 2:

$$F_{\mathrm{cap},2} = \frac{\gamma_2 V_{\mathrm{m}}/V q_{\mathrm{sat}} bRT}{(1+0.5bP_{\mathrm{ex}})^2} \tag{18}$$

Accordingly we obtain the mobility enhancement factor:

$$F_{\mathrm{diff},2} = \frac{\gamma_2(1-\varepsilon) q_{\mathrm{sat}} bRTD_{\mathrm{S},2}/D_{\mathrm{K},2}}{1+0.5bP_{\mathrm{ex}}} \tag{19}$$

where $D_{\mathrm{s},2}$ is the surface diffusion coefficient and $D_{\mathrm{K},2}$ is the Knudsen diffusion coefficient. It should be noted that the factor γ_2 is a fitting parameter. It is required that this value is in the range between 0 and 1 since it is the volume fraction of the membrane which is saturated.

It may be worthwhile to mention, that capacity enlargement and mobility enhancement can partly compensate each other. If both extension functions exhibit the same amount, then the pressure response would be the same as the one for a pure Knudsen type membrane.

3.2.2.2. Case 2.2:two adsorbable gases. If adsorption occurs to both components 1 and 2, like for the CO_2/C_3H_8 system, the relaxation times of components $i=1, 2$ is given by Eq. (14b), with

$$F_{\mathrm{cap},i} = \frac{\gamma_i V_{\mathrm{m}}/V q_{\mathrm{sat}} bRT}{(1+0.5bP_{\mathrm{ex}})^2} \tag{20}$$

$$F_{\mathrm{diff},i} = \frac{\gamma_i(1-\varepsilon) q_{\mathrm{sat}} bRTD_{\mathrm{S},i}/D_{\mathrm{K},i}}{1+0.5bP_{\mathrm{ex}}} \tag{21}$$

Numerical values of the γ_i depend on the sorption isotherms of both components of the gas mixtures. Since those are currently not available such an evaluation has been omitted below.

4. Results and discussions

Below the results of several experiments will be reported in comparison with the theoretical model leading to Eq. (12).

4.1. Non-adsorbable gases (He/N_2)

The pore diameter of Vycor glass (about 4 nm) is sufficiently smaller than the mean free path λ of He, and N_2 at 20 °C and at 1 bar. Thus the transfer of non-adsorbable gases is considered to be governed by Knudsen diffusion through the membrane. Provided the characteristic constant of K_0 is known, using Eq. (14a), the Knudsen relaxation times $t_{i,\mathrm{k}}$ can be calculated.

Using $K_0 = 7.08\mathrm{E}{-11}$ m, which was determined by a state-steady permeation experiments in previous work [6], the predicted $t_{1,\mathrm{k}}$ and $t_{2,\mathrm{k}}$ are 33.37 and 88.29 s, respectively. In Fig. 3, the relaxation time fitted Eq. (12) to the measured transients are compared to these calculated ones. There is a good consistency between the fitted and calculated ones. The ratio of the two fitted $t.1$ and $t.2$ is almost equal to the reverse of square root of molar mass, $(M_2/M_1)^{0.5}$. It confirms the Knudsen diffusion mechanism for inert gases, and it also indicates the good validation of the parameter estimate for K_0.

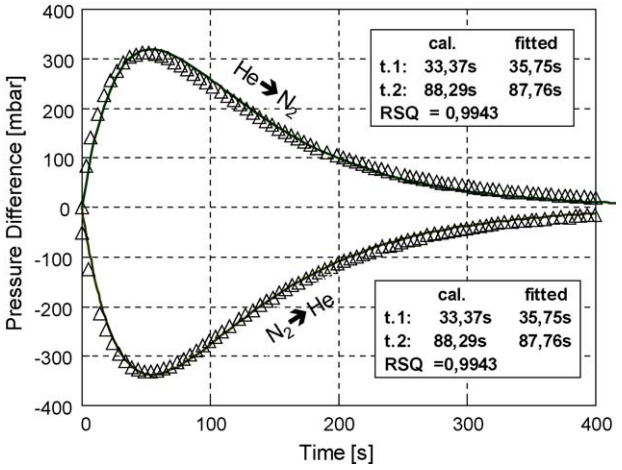

Fig. 3. Comparison between calculated and fitted results for transient diffusion of He/N_2 system ((△)observations; (—) fitted curve).

4.2. Transients for inert (1)–adsorbable (2) gases (He/C_3H_8 and He/C_4H_{10})

These are systems where one component is non-adsorbable, whereas the other one is adsorbable. Again, the relaxation times $t.1$ and $t.2$ in Eq. (12) were fitted to the experimental data and compared to the Knudsen ones.

4.2.1. The fitted and predicted relaxation time of each component for transients of He/C_3H_8

In Fig. 4 are shown the observed and fitted transients for exchange experiments with He/C_3H_8. There is a pronounced asymmetry between two reversed exchange experiments instead of the symmetry observed for He/N_2 gases, as seen in Fig. 3. Eq. (12) gives a good fit to the observations with excellent accuracy of RSQ, 0.9943 and 0.9963 for He substituting C_3H_8 and the reverse experiment, respectively.

The fitted relaxation time for C_3H_8: $t.2 = 153.08$ or 154.08 s is different from the Knudsen relaxation time, which is $t_{2,k} = 93.06$ s. A reasonable value of 0.4 is obtained for γ_2 by fitting Eq. (18) to the obtained relaxation time $t.2$ using the adsorption isotherm of C_3H_8 and the surface diffusion coefficient values as presented in the previous work [6]. The question how to predict the parameter γ_2 is a subsequent task beyond the present approach.

For He the fitted relaxation time $t.1$ is practically equal to the Knudsen one, $t_{1,k} = 33.37$ s if C_3H_8 replaces He. However, the fitted relaxation time $t.1$ of 44.04 s is larger than $t_{1,k}$ when He replaces C_3H_8. This is probably due to the fact that the C_3H_8 molecules preadsorbed at the pore walls reduce the effective pore size, resulting in a decrease of the permeability according to Eq. (14a). Assuming a monolayer of adsorbed C_3H_8 molecules with 0.43 nm diameter [12], the effective pore diameter is reduced to about 3 nm from 4 nm, thus giving a relaxation time of 44.04 s according to Eq. (14a). In the reverse exchange, i.e. C_3H_8 replaces He, most of the He molecules pass the membrane before the adsorption layer was formed at the pore walls, and therefore no reduction of the permeability for He did occur.

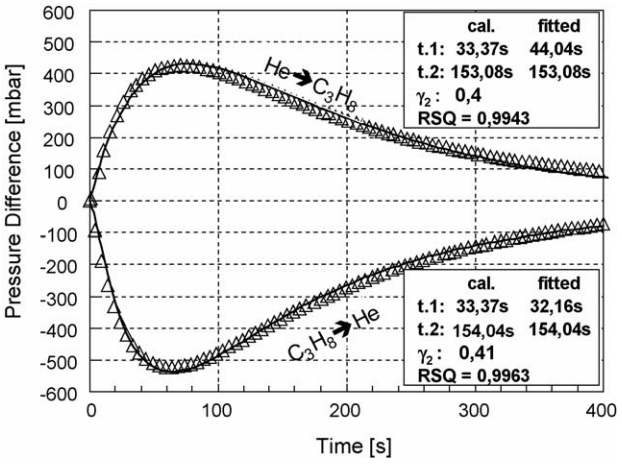

Fig. 4. Comparison between calculated and fitted results for transient diffusion of He/C_3H_8 system (△) observations; (—) fitted curve).

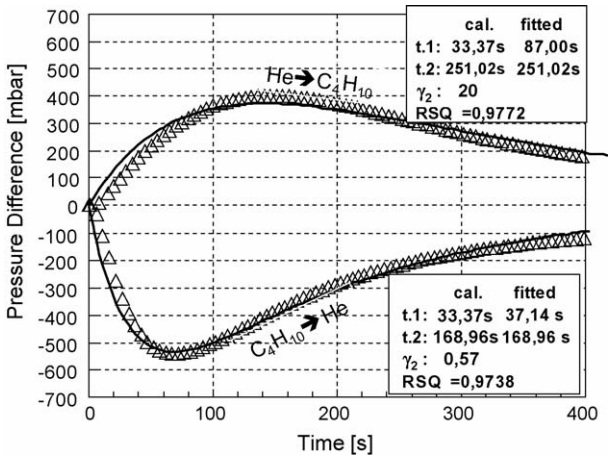

Fig. 5. Comparison between calculated and fitted results for transient diffusion of He/C_4H_{10} system ((△) observations; (—) fitted curve).

4.2.2. The fitted and predicted relaxation times for transients of He/C_4H_{10} gases

In Fig. 5 are shown the observed and fitted transients at 20 °C for He/C_4H_{10} exchange experiments. The asymmetry is equally found between the two inverse exchange experiments as in the experiments for He/C_3H_8 discussed above. Eq. (12) shows a good match to the observed transients with relatively high RSQ of 0.9772 and 0.9738, respectively.

When He replaces C_4H_{10}, the fitted relaxation time $t.1$ for He is 87 s and thus about three times larger than the one for Knudsen diffusion. The fitted relaxation time $t.2$ for C_4H_{10} is 251.02 s and requires a fitted saturation capacity factor γ_2 of 20, which is an unreasonable value.

When C_4H_{10} replaces He, the fitted $t.1$ is 37.14 s, and only slightly different from $t_{1,k.}$ Fitting the relaxation time $t.2$ of 168.96 s, requires a saturation capacity factor γ_2 of 0.57, which is a reasonable value.

The reason, why the fitted capacity factor γ_2 is much larger than 1 and the permeability of He is strongly reduced when He replace C_4H_{10}, compared to the one when He replaces C_3H_8, is probably due to the appearance of capillary condensation of C_4H_{10}, causing a blocking of a considerable part of the open pores.

4.3. Two adsorbable gases (C_3H_8/CO_2)

Combination of gases like C_3H_8/CO_2 are of particular interest since the molar masses of C_3H_8 and of CO_2 are equal and, therefore, no pressure response should be observed if the gas permeation would be governed by Knudsen diffusion alone.

Therefore, the large pressure responses observed in our experiments – for various temperatures or compositions – were due to the competitive adsorption and surface diffusion.

4.3.1. Temperature dependency of the pressure response

The pressure responses for the system C_3H_8/CO_2 at various temperatures are shown in Fig. 6. As can be seen, the amplitude of the pressure responses decreases with increasing temperatures, from around 160 and −240 mbar at 20 °C, respectively,

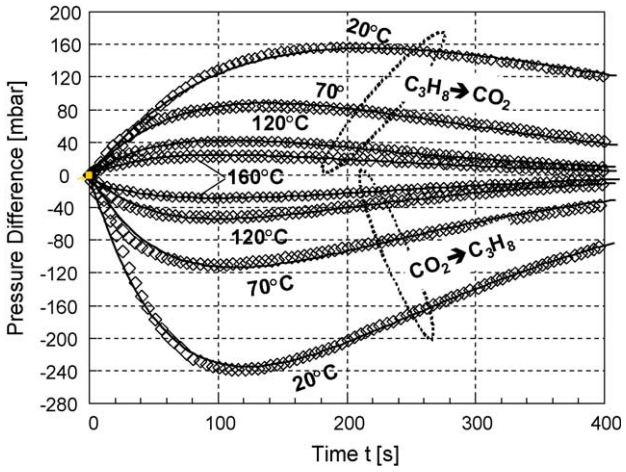

Fig. 6. Comparison between calculated and fitted results for transient diffusion of C_3H_8/CO_2 system at various temperatures ((◇) observations; (—) fitted curve).

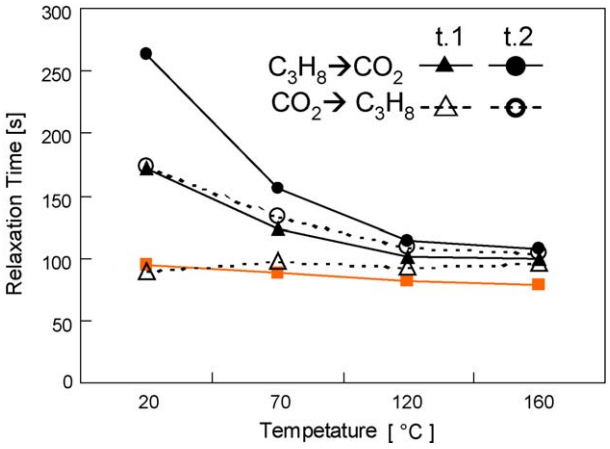

Fig. 7. Dependency of relaxation time on the temperature ((▲) fitted relaxation time of C_3H_8; (●) fitted relaxation time of CO_2; (■) calculated Knudsen relaxation time; solid curve: transient of C_3H_8 replacing CO_2; dashed curve: transient of CO_2 replacing C_3H_8).

to around 30 and −30 mbar at 160 °C. The asymmetry between the two reverse exchange experiments becomes weaker with increasing temperatures. These results are to be expected since the amount of adsorbed molecules decreases as temperature increases. At sufficiently high temperatures the pressure response should go to zero.

It should be noted, that the relaxation time of C_3H_8 was found to be shorter than the one for CO_2.

Eq. (12) surprisingly matches to all observations made despite of the simplified description of the adsorption behaviour of the two adsorbable gases. The lowest RSQ obtained among these fittings is 0.9795. The fitted relaxation times, $t.1$ for C_3H_8 and $t.2$ for CO_2 are summarized in Table 1. The values of $t.1$ and $t.2$ are much larger than those for the Knudsen ones, $t_{1,k}$ and $t_{2,k}$ at low temperature of 20 °C and approach gradually to the Knudsen ones at higher temperatures (Fig. 7).

4.3.2. Composition dependency of the pressure response

Fig. 8 shows the pressure response for systematic exchange experiments of various mixtures with an initial partial pressure difference of 0.2 bar between C_3H_8 and CO_2 and vice versa. Fig. 9 shows the corresponding responses for mixtures with the initial partial pressure difference of 0.5 bar.

Again Eq. (12) can surprisingly fit to all these observations with sufficiently good accuracy. The fitted $t.1$ and $t.2$ are listed in Tables 2 and 3. Knowledge regarding the adsorption behaviour of mixtures is required for the understanding of these fitted time constants. Adsorption measurements for the mixtures will be performed using a volumetric method as used in our previous work [4].

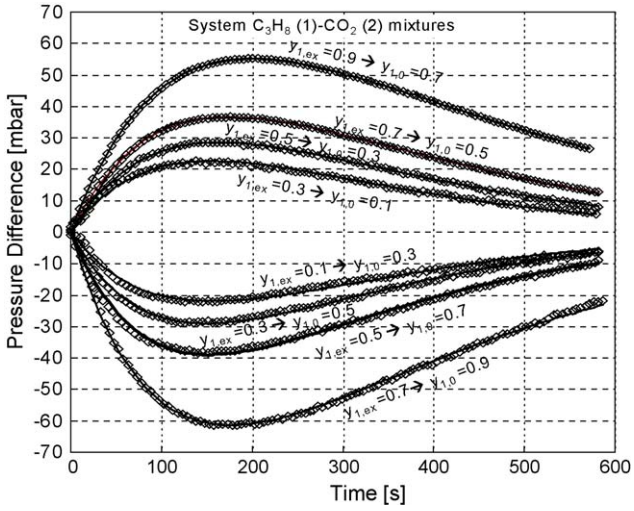

Fig. 8. Fitted and observed transients for C_3H_8/CO_2 mixtures varying composition ratio ($\Delta P_0 = 0.2$ bar) ((◇) observations; (—) fitted curve).

Table 1
Fitted relaxation times of $t.1$, and $t.2$ for C_3H_8 replacing CO_2 and vice versa at various temperatures

Temperature (°C)	$C_3H_8 \rightarrow CO_2$				$CO_2 \rightarrow C_3H_8$			
	$t.1$ (s)	$t.2$ (s)	RSQ	Mean deviation (%)	$t.1$ (s)	$t.2$ (s)	RSQ	Mean deviation (%)
20	171.2	262.5	0.9951	1.49	90.0	172.5	0.9971	0.97
70	122.8	156.0	0.9887	2.57	97.2	132.5	0.9865	3.07
120	101.6	114.1	0.9884	3.71	93.8	108.7	0.994	2.31
160	100.1	107.1	0.9795	5.90	96.9	105.0	0.9859	3.34

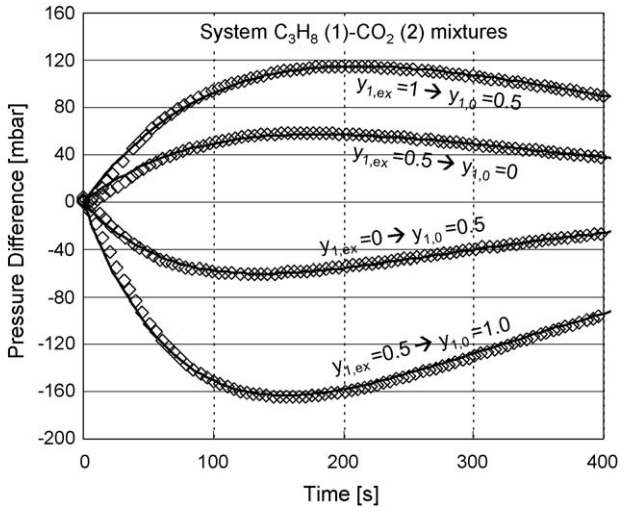

Fig. 9. Fitted and observed transients for C_3H_8/CO_2 mixtures varying composition ratio ($\Delta P_0 = 0.5$ bar) ((◇) observations, (—) fitted curve).

mechanism, taking into account that the effective pore diameter may be reduced due to an adsorbed monolayer of C_3H_8 in case that He replaces C_3H_8, while this reduction does not take place, if C_3H_8 replaces He.

The same behaviour – but much more severe – was observed with the gas combination He/C_4H_{10}. In this case the pore size reduction was caused not only by the formation of monolayer but by the onset of capillary condensation, with an absolute blockage effect.

For the gas combination C_3H_8/CO_2, showing equal molar masses, the pure Knudsen type pressure response vanishes. The observed pressure responses were solely due to adsorption effects—storage and surface diffusion. At higher temperatures adsorption disappears and – as expected – the pressure response, too. The dependence of the pressure response on the composition shows a certain tendency of the fitted relaxation times with mixture composition.

An independent approach for the determination of the relaxation times is required to render the model predictive. In future a frequency response technique will be applied to further study the system considered and to quantify in more detail the observations. It is expected that this approach will also allow estimating adsorption isotherms for mixtures.

Table 2
Fitted relaxation times (Eq. (12)) of C_3H_8 (1) and CO_2 (2) for C_3H_8–CO_2 mixtures with systematically varying composition ratio at 20 °C ($\Delta p = 0.2$ bar)

Gas system	C_3H_8 (1): CO_2 (2) → C_3H_8 (1): CO_2 (2), $y_{1,ex} \rightarrow y_{1,0}$							
	0.9 → 0.7	0.7 → 0.5	0.5 → 0.3	0.3 → 0.1	0.1 → 0.3	0.3 → 0.5	0.5 → 0.7	0.7 → 0.9
t.1 (s)	139.5	138.2	136.4	133.4	134.9	123.6	118.0	118.4
t.2 (s)	300.8	228.4	201.4	181.4	181.8	182.9	201.5	297.4
RSQ	1.0	0.9973	0.9977	0.9954	0.9853	0.9955	0.9959	0.9984
Deviation (%)	0	0.92	0.90	1.70	2.87	1.49	1.60	0.79

Table 3
Fitted relaxation times (Eq. (12)) of C_3H_8 (1) and CO_2 (2) for C_3H_8–CO_2 mixtures with systematically varying composition ratio at 20 °C ($\Delta p = 0.5$ bar)

Gas system	C_3H_8 (1):CO_2 (2) → C_3H_8 (1):CO_2 (2), $y_{1,ex} \rightarrow y_{1,0}$			
	1 → 0.5	0.5 → 0	0 → 0.5	0.5 → 1
t.1 (s)	156.4	154.9	116.3	101.64
t.2(s)	295.3	217.7	161.6	254.55
RSQ	0.9964	0.9971	0.9968	0.9955
Deviation (%)	0.98	0.43	0.43	1.61

5. Conclusion

The suggested lumped two parameter approach, Eq. (12), is found simple and capable of fitting a large amount of experimental data regarding mass transfer in a porous Vycor glass membrane studied in a transient diffusion experiment with sufficient or excellent accuracy.

For inert gases like He/N_2 the fitted relaxation times *t*.1 and *t*.2 are in perfect agreement with the predicted ones based on the assumption of pure Knudsen diffusion.

For the adsorbable gases, like CO_2 and C_3H_8, the relaxation times must include additional effects due to the storage capacity enlargement and the permeability enhancement resulting from surface diffusion.

For the gas combinations He/C_3H_8, the relaxation time of the inert gas He follows from the Knudsen type diffusion

Appendix A

Langmuir adsorption isotherm data and surface diffusion coefficient at 20 °C were taken from Ref. [6].

	Saturation load q_{sat} (mol/cm^3)	b (bar^{-1})	$D_{s,i}$ (m^{2}s^{-1})
C_3H_8	1.15E−3	0.965	3.10E−9
CO_2	3.15E−3	0.467	2.20E−9

References

[1] H.P. Hsieh, Inorganic Membranes for Separation and Reaction, Membrane Science and Technology, vol. 3, Elsevier, Amsterdam, 1996.
[2] J.G. Sanchez Marcano, T.T. Tsotsis, Catalytic Membranes and Membrane Reactors, Wiley–VCH, Weinheim, 2002.
[3] A. Seidel-Morgenstern, Analysis and experimental investigation of catalytic membrane reactors, in: K. Sundmacher, A. Kienle, A. Seidel-Morgenstern (Eds.), Integrated Chemical Processes, Wiley–VCH, Weinheim, 2005.
[4] J. Yang, J. Čermáková, P. Uchytil, C. Hamel, A. Seidel-Morgenstern, Gas phase transport, adsorption and surface diffusion in a porous glass membrane, Catal. Today 104 (2005) 344–351.
[5] A. Tuchlenski, Charakterisierung poröser Membranen und ihre Charakterisierung in Membranreaktoren, Ph.D. thesis, Otto-von-Guericke-Universität Magdeburg (1998) and Logos Verlag Berlin, ISBN 3-89722-145-4, 1998.
[6] A. Tuchlenski, P. Uchytil, A. Seidel-Morgenstern, An experimental study of combined gas phase and surface diffusion in porous glass, J. Membr. Sci. 140 (1998) 165.
[7] M. Novak, K. Ehrhardt, K. Klusacek, P. Schneider, Dynamics of non-isobaric diffusion in porous catalysts, Chem. Eng. Sci. 43 (1988) 185.
[8] H.D. Do, D.D. Do, I. Prasetyo, Surface diffusion and adsorption of hydrocarbons in activated carbon, AIChe J. 47 (11) (2001) 2515–2525.
[9] M. Dogan, G. Dogu, Dynamics of flow and diffusion of adsorbing gases in Al_2O_3 and Pd–Al_2O_3 Pellets, AIChe J. 49 (12) (2003) 3188–3198.
[10] R. Krishna, Problems and pitfalls in the use of the Fick formulation for intraparticle diffusion, Chem. Eng. Sci. 48 (1993) 845.
[11] J.O. Hirschfelder, C.F. Curtiss, R.B. Bird, Molecular Theory of Gases and Liquids, John Wiley & Sons, Inc., 1964.
[12] D.W. Breck, Zeolite Molecular Sieves, Wiley, New York, 1974.